

## The effect of direction for hydrophobic lines on subcooled flow boiling: Critical heat flux and heat transfer coefficient

Jin Man Kim<sup>a</sup>, Dong In Yu<sup>a</sup>, Hyun Sun Park<sup>a\*</sup>, Moo Hwan Kim<sup>a,1</sup>

<sup>a</sup>Division of Advanced Nuclear Engineering, POSTECH, Pohang 790-784, Gyungbuk, Republic of Korea

\*Corresponding author: [hejsunny@postech.ac.kr](mailto:hejsunny@postech.ac.kr)

<sup>1</sup>Currently working in Korea Institute of Nuclear Safety (KINS) as a president

### 1. Introduction

Two phase boiling heat transfer is an efficient method to deliver energy. Specially, flow boiling shows better boiling heat transfer than one in pool boiling due to convective effect. For this reason, many applications have adopted flow boiling like nuclear power plant. In the two phase system, heat transfer coefficient (HTC) and critical heat flux (CHF) are the main interests that represent efficiency and operational limitation of the system. Therefore, a lot of time and effort were dedicated on study of BHT and CHF to understand and control boiling characteristics.

To enhance boiling performance, structure and coating have been focused on recently. Coating can change wettability of the surface by controlling surface energy. Structure can affect nucleation cavity or wettability. These techniques make differences for boiling phenomena. From many reports, structures have received much attention due to facileness of manipulation for wetting, and so much data were collected about structures and boiling characteristics. In comparison to the structure, the study of coating technique is less active. Hydrophilic surface without structure is difficult to make for lasting during boiling condition, and hydrophobic surface impoverish CHF due to early dryout. For this reason, the study of coating effect is deficient relatively. However, hydrophobic pattern can be a brilliant method to enhance boiling performance. Betz *et al.* [1] manufactured superbiphilic surfaces having juxtaposing hexagonal hydrophobic dots on the superhydrophilic surface. This surface improved HTC up to three times higher than on reported nanostructured surfaces. They reported that results were from increasing nucleation site due to hydrophobicity and constraining of bubble expansion on the surface to prevent formation of vapor blanket.

In this study, hydrophobic patterns with stripe lines were achieved to study direction effect of hydrophobic pattern using Teflon solution, and further research is suggested.

### 2. Experiments

To study flow boiling characteristics on hydrophobic lined surfaces, rectangular channel was used with

POSTECH flow boiling loop. All experiments were conducted in subcooled and at low pressure condition.

#### 2.1. Flow boiling loop

Fig. 1 shows POSTECH flow boiling loop which uses DI water as a working fluid. DI water circulates closed loop through flow meter, preheater, test channel and condenser. The mass flux is controlled using two valves: main valve and bypass valve. At the condenser, heated DI water is cooled down with counter flow heat exchange with tap water through secondary loop. Preheater is used to control inlet temperature of DI water and for degassing process. Flow meter is positioned before preheater to prevent thermal damage, and used to calculate mass flux. At the inlet and outlet of the test channel, temperature and pressure are measured.

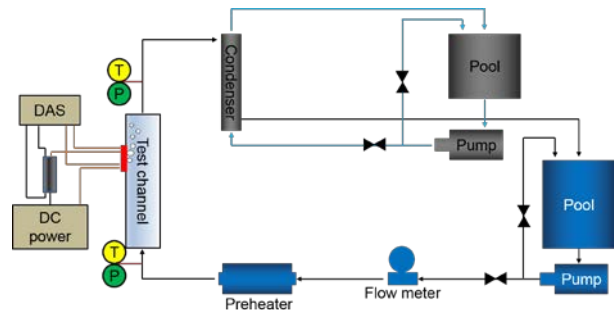


Fig. 1. Flow boiling loop

#### 2.2. Test channel

Test channel is rectangular and vertical upward directional. The hydraulic diameter is 7.5 mm which is macro-meter scale channel from analysis of [2]. With considering entrance length, heater was fixed at 240 mm from the inlet.

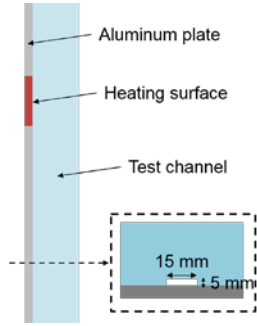


Fig. 2. Test channel

### 2.3. Test section

Silicon wafer was adopted as a heating surface to minimize structure effect. The roughness of silicon was about 1 nm scale, so it's reasonable to think silicon wafer as an ideal smooth surface based on classical cavity theory [3].

In this study, Teflon coated surface without pattern was a reference for the comparison. On the back side of the silicon wafer (thickness was 500 μm), platinum (Pt) layer of 120 nm was patterned for Joule heating in Fig. 3. On the other side, SiO<sub>2</sub> layer of 500 nm was deposited using thermal growth for insulation. After SiO<sub>2</sub> layer was deposited, measured roughness was about 1 nm, so this layer didn't change surface morphology. To make different wetting pattern, Teflon was coated or patterned using spin coater. Contact angles of SiO<sub>2</sub> and Teflon were 56.8 ° and 120.4 ° respectively.

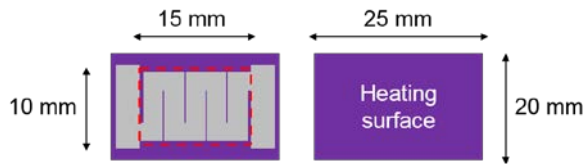


Fig. 3. Test section

The mask of the stripe lines was made with 1 mm line spacing before spin coating. From the direction of the lines, they were named to cross and parallel in Fig. 4.

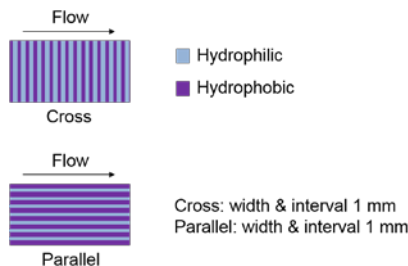


Fig. 4. Teflon patterns

### 2.4. Uncertainties

Table I. shows experimental ranges and uncertainties. For experiments, hydrophobic lines were controlled to study these effect on boiling characteristics. Here, heat flux was calculated from measured voltage and calculated current data using (1). In the test section circuit, DC power was supplied through reference resistance which maintained constant temperature to make constant resistance value. Measured voltage drop at reference resistance was measured to calculate current of the circuit with resistance value. During experiment, voltage drop at heating element was measured. Using voltage drop and current, heat flux was calculated in real time. From the analysis of Coleman [4], uncertainty of heat flux could be estimated by (2).

$$q'' = \frac{V_{heater} \times V_{ref}}{R_{ref} \times A_{heater}} \quad (1)$$

$$\frac{U_{q''}}{q''} = \sqrt{\frac{U_{V_{heater}}^2}{V_{heater}^2} + \frac{U_{V_{ref}}^2}{V_{ref}^2} + \frac{U_{R_{ref}}^2}{R_{ref}^2}} \quad (2)$$

Table I: Experimental range and uncertainties

Parameter	Range	Uncertainty
Hydraulic diameter (mm)	7.5	0.057 (0.755 %)
Mass flux (kg/m <sup>2</sup> s)	600	6.353 (1.059 %)
Inlet pressure (kPa)	170-300	37.921 (12.640 %)
Inlet, outlet temperature (°C)	98	1 (1.020 %)
Wall temperature (°C)	170	0.3 (0.176 %)
Heat flux (kW/m <sup>2</sup> )	50-1500	8.651 (0.584 %)

### 2.5. Experimental step

Before experiments, the resistance of Pt pattern was correlated with different temperature condition in the

convection oven. Using this correlation, temperature of test section could be measured during experiment.

Before every experiment, DI water was degassed using preheater for 1 hour. During experiment, heat flux was increased step-wisely and maintained for 2 minutes at targeted heat flux with regarding steady-state condition. When abrupt increase of temperature was detected, then experiment was stopped and this point was defined as a CHF point. After CHF point, HTC was decreased rapidly.

### 3. Results and discussion

#### 3.1. Critical heat flux

Fig. 5 shows boiling curves for all surfaces. Teflon means smoothly coated surfaces on the whole area by Teflon solution without pattern and cross and parallel means line direction to the flow. G and T are mass flux ( $\text{kg/m}^2\text{s}$ ) and inlet temperature ( $^{\circ}\text{C}$ ) respectively. From the experiments, the CHF values are  $562 \text{ kW/m}^2$ ,  $1186 \text{ kW/m}^2$ ,  $1481 \text{ kW/m}^2$  for Teflon, cross, parallel.

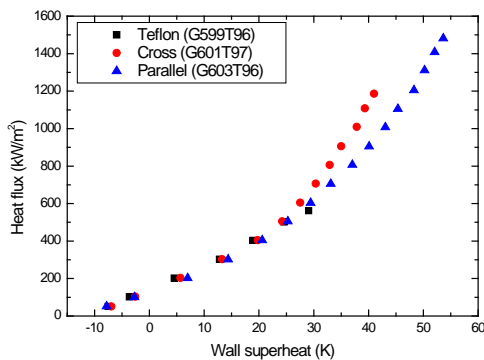


Fig. 5. Boiling curves

In detail, Teflon coated surface had the lowest CHF, and parallel pattern showed the highest CHF. These results can be explained phenomenologically. Teflon made many bubbles at the low heat flux. On the Teflon coated surface, too many bubbles were generated at  $600 \text{ kW/m}^2$ , so vapor blanket appeared very early stage causing CHF.

On the parallel patterned surfaces, water could be supplied to the dried area through non-coated line by flow. So, it's advantageous to delay CHF. On the cross patterned surfaces, CHF was lower than the values of parallel pattern. These results were attributed to impediment of water supply to the heating surface. On the contrary to parallel pattern, flow pushes vapor to the flow direction across the different wetting patterns. During this process, water supply on the hydrophilic lines was disturbed by vapor sweeping. Because there was no external force to supply water in the orthogonal

direction to the flow, CHF on the cross patterns was decreased due to deficiency water supply.

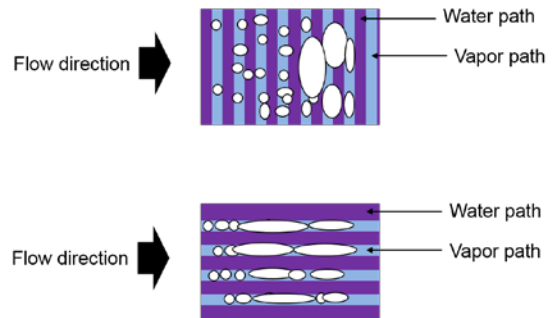


Fig. 6. Mechanism of CHF

#### 3.2. Heat transfer coefficient

Fig. 7. Shows HTCs versus wall superheat for each surface. In this research, heat transfer region could be divided into two region, low wall superheat and high wall superheat by below  $20 \text{ K}$  and above  $30 \text{ K}$  respectively. The trends of HTCs were totally different at each region. Between  $20 \text{ K}$  and  $30 \text{ K}$ , there were transitions of bubble dynamics which is not the interest in this research.

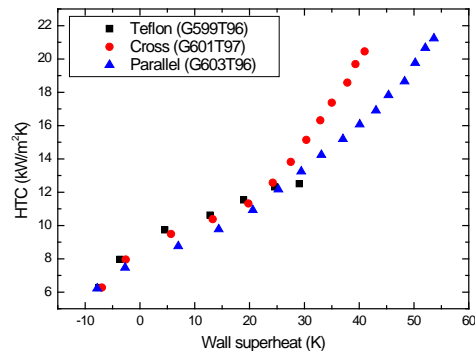


Fig. 7. HTC versus wall superheat

At the low wall superheat region, Teflon showed the best HTC because it had the largest hydrophobic area, but it couldn't be lasted above high wall superheat region due to formation of vapor blanket. On the patterned surface, bubble frequency ( $f$ ) and the drag ( $F_D$ ) were the major parameters for HTC. Generally, drag is expressed in (3), where  $\rho$ ,  $v$ ,  $C_D$ ,  $A$  are density of liquid ( $\text{kg/m}^3$ ), the relative speed to the fluid (m/s), drag coefficient, cross sectional area ( $\text{m}^2$ ) respectively. From the equation, drag is proportional to the cross sectional area. In Fig. 8, on the each patterned surface, bubble shapes were assumed to simplified rectangular shape from the top view. Then, for the one

merged elongated vapor, drag is proportional to the width of elongated bubble like in (4), where  $W$  is width (m). For the elongated bubbles on each pattern, all parameters were same except  $W$ . Then, larger drag is applied to the wide bubble on the cross patterned surface. Thus, vapor bubbles on the cross patterns could be broken up easily and departed earlier than the ones on the parallel patterns. It accelerated bubble departure frequency,  $f$ , causing higher HTC. It's the main reason for higher HTC.

$$F_D = \frac{1}{2} \rho v^2 C_D A \quad (3)$$

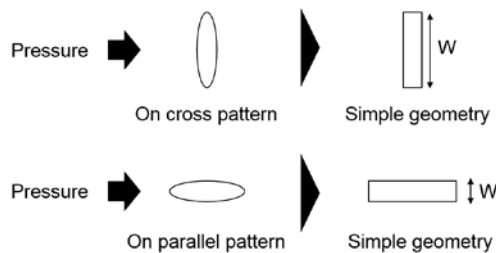


Fig. 8. Assumption of bubble shape

$$F \sim W \cdot f(\rho, v, C_D, H) \quad (4)$$

At the high wall superheat region, more bubbles were generated. Thus, the more bubbles were generated, the more bubbles break up on the cross patterned surface. Vigorous bubbles were generated on the hydrophobic lines and broken up or departed from the surface due to the flow, so HTC on cross pattern was more enhanced at the high wall superheat region. However, on the parallel patterned surface, bubbles were more elongated than broken up or departed from the hydrophobic lines. In this reason, cross pattern was favorable to enhance HTC.

#### 4. Conclusions

From the analysis of bubble dynamics with pattern effects, the following conclusions can be summarized.

1. Teflon coating can make many bubbles at early stage, so it showed the highest HTC, but lowest CHF due to early formation of vapor blanket.
2. Parallel patterns are advantageous higher CHF due to segregated vapor path in flow direction.
3. Cross patterns are unfavorable to delay CHF because merged vapor jets could cover hydrophilic line.
4. Parallel patterns have no advantage for HTC because there was little bubble break up.

5. On the cross patterns, larger drag made vigorous bubble break up, so HTC was increased.

In addition, the following further research is suggested.

1. The study of width effect for hydrophobic line.
2. The study of interval effect for hydrophobic lines.
3. Integrated patterns are potential surface to enhance both HTC and CHF.

#### ACKNOWLEDGEMENTS

This work was also supported by National Research Foundation of Korea (NRF) grants funded by the Korean government (MSIP) (NRF-2014M2B2A9031122)

#### REFERENCES

- [1] A. R. Betz, J. Jenkins, C.-J. “CJ” Kim, and D. Attinger, Boiling heat transfer on superhydrophilic, superhydrophobic, and superbiphilic surfaces, *International Journal of Heat and Mass Transfer*, Vol. 57, No. 2, pp. 733–741, 2013.
- [2] C. L. Ong and J. R. Thome, Macro-to-microchannel transition in two-phase flow: Part 1—Two-phase flow patterns and film thickness measurements, *Experimental Thermal and Fluid Science*, Vol. 35, No. 1, pp. 37–47, 2011.
- [3] S. G. Bankoff, Entrapment of gas in the spreading of a liquid over a rough surface, *AIChE Journal*, Vol. 4, No. 1, pp. 24–26, 1958.
- [4] H. W. Coleman and W. G. Steele, *Experimentation, validation, and uncertainty analysis for engineers*. John Wiley & Sons, 2009.